Migraine eye: correlation between migraine and the retina

Lunla Udomwech[1], Rini Sulastiwaty[2] and Doungkamol Siriarchawawat[3]

[1] Department of Ophthalmology, School of Medicine, Walailak University, Thasala, Nakhonsithammarat, Thailand
[2] Glaucoma Service, Jakarta Eye Center, Jakarta, Indonesia
[3] Division of Neurology, Department of Internal Medicine, School of Medicine, Walailak University, Thasala, Nakhonsithammarat, Thailand

ABSTRACT

Background: Activation of the trigeminal vascular system in migraine releases vasoactive neurotransmitters, causing abnormal vasoconstriction, which may affect the ocular system, leading to retinal damage. The purpose of our study was to determine whether there are differences in each retinal layer between migraine patients and healthy subjects.

Methods: A case-control study recruited 38 migraine patients and 38 age- and sex-matched controls. Optical coherence tomography was used to measure the thickness of the peripapillary and macular retinal nerve fiber layer (pRNFL and mRNFL), ganglion cell layer (GCL), inner plexiform layer (IPL), and inner nuclear layer (INL).

Results: The mean ages of the migraine patients and controls were 36.29 ± 9.45 and 36.45 ± 9.27 years, respectively. Thirty-four patients (89.48%) in both groups were female. The mean disability score was 19.63 ± 20.44 (indicating severe disability). The superior-outer INL of migraine patients were thicker than controls. Thickness of the GCL at temporal-outer sector and mRNFL at the superior-outer sector of the headache-side eyes was reduced. However, the INL of the headache-side-eye showed negative correlation with the disability score. This is the first study having found thinning of the GCL and mRNFL of the headache-side eyes. The INL was also thickened in migraines but showed negative correlation with the disability score.

Conclusions: Increased INL thickness in migraine patients may result from inflammation. The more severe cases with a high disability score might suffered progressive retinal neuronal loss, resulting in thinner INL than less severe cases.

Subjects Neuroscience, Neurology, Ophthalmology, Radiology and Medical Imaging
Keywords Retinal nerve fiber layer, Ganglion cell layer, Inner nuclear layer, Migraine, Optical coherence tomography, Thickness

INTRODUCTION

Migraine is a common primary headache disorder that affects patients worldwide. The prevalence among the Thai population is 29.1%, which is higher than that in the United States (11.7%) (*Phanthumchinda & Sithi-Amorn, 1989*). Migraine is characterized by recurrent attacks of throbbing, unilateral, and usually severe headaches (*Headache Classification Committee of the International Headache Society, 2018*). The understanding

of migraine pathophysiology has drastically improved in the last two decades. It is generally accepted that migraine attacks occur through the activation and sensitization of the trigeminal vascular system (TGVS) (*Russo, Tessitore & Tedeschi, 2013*). This activation releases pain-producing vasoactive neurotransmitters, causing abnormal vasoconstriction and aura symptoms when this phenomenon occurs in the occipital lobe.

Using optical coherence tomography (OCT), several studies have shown that vascular changes also occur in the ocular system during migraine attacks (*Killer, Forrer & Flammer, 2003*; *Abdul-Rahman, Gilhotra & Selva, 2011*). Vasoconstriction can cause damage to the retinal nerve fiber layer (RNFL) and retinal ganglion cell layer (GCL) (*Lin et al., 2021*), detectable by the thinning of these layers from OCT, although the results of such studies are discrepant. The purpose of our study was to determine whether there are differences in retinal thickness between migraine patients and healthy subjects. In migraine group, we evaluate RNFL thickness on the side of the headache (headache-side eye) compared to contralateral side (non-headache-side eye) and evaluate the thicknesses of the nasal and temporal sides of each eye in respect to the optic pathway. We measured the thickness of the peripapillary retinal nerve fiber layer (pRNFL), macular retinal nerve fiber layer (mRNFL), ganglion cell layer (GCL), inner plexiform layer (IPL), and inner nuclear layer (INL) using OCT to assess the correlation between these structural changes and migraine parameters, including disease duration, attack frequency per month, and disability score (Thai-MIDAS; the Thai version of Migraine Disability Assessment score).

MATERIALS AND METHODS

Participants: this cross-sectional descriptive study was conducted at Walailak University Hospital (Nakhon Si Thammarat, Thailand) between July 2021 and August 2022. This prospective study was approved by the Walailak Ethics Committee (WUEC-21-166-01). Written informed consent was obtained from all participants after a full explanation of the study. This study complied with the principles of the Declaration of Helsinki and the International Conference on Harmonization of Good Clinical Practice.

We recruited migraine patients with and without aura who were diagnosed by a neurologist at the neurology outpatient clinic. All patients met the migraine diagnosis according to the criteria of the International Classification of Headache Disorders (ICHD-3 beta) (*Headache Classification Committee of the International Headache Society (IHS), 2013*). Migraine disability scores were assessed by a neurologist using a migraine disability questionnaire: Migraine Disability Assessment Score Thai Version (Thai-MIDAS), developed by *Vongvaivanich et al. (2018)*. Patients were interviewed about the type of migraine (with or without aura), the pattern of aura, duration of migraine history, the number of attacks per month (in the previous three months), antimigraine medication, impact of headaches on daily life, and pain severity scores. The Thai-MIDAS scores were divided into four grades: grade I, infrequent disability; grade II, mild disability; grade III, moderate disability; and grade IV, severe disability. We excluded patients with previous retinal disorders, glaucoma, previous ocular surgery/laser, and disorders of the cornea or lens that prevented the ophthalmologist from evaluating retinal thickness precisely.

The control group consisted of age- and sex-matched healthy controls (HCs) who were chosen prospectively and reported either fewer than three headaches in the past year or headaches not meeting the migraine ICHD-3 beta criteria. The exclusion criteria were a history of central nervous system disorders and ocular disorders as mentioned above.

Ophthalmic evaluation and OCT: all participants underwent a full ophthalmic examination by an ophthalmologist, including best-corrected visual acuity (BCVA) measured by the Early Treatment Diabetic Retinopathy Study (ETDRS) chart, intraocular pressure (IOP) measured by the iCare tonometer (Finland Oy, Vantaa, Finland), pupil size and reactivity, slit lamp examination, and fundus examination by BQ-900 slit lamp biomicroscope (Haag-Streit, Berne, Switzerland) at the ophthalmology clinic of Walailak University Hospital.

OCT was performed without pupillary dilatation with the SPECTRALIS OCT2 Module (Heidelberg, Heidelberg, Germany). The image quality was assessed. The measurement of peripapillary RNFL included six sextants from each eye: temporal, nasal, temporal superior, nasal superior, temporal inferior, and nasal inferior. The GCL thickness, macular RNFL thickness, IPL thickness, and INL thickness were divided into eight regions according to ETDRS: temporal-inner, superior-inner, nasal-inner, inferior inner, temporal-outer, superior-outer, nasal-outer, and inferior-outer.

Both eyes of each participant were included for comparison of parameters between the migraine and healthy control groups. The sample size calculation was based on a study by *Tunç et al. (2017)* using the two independent means equation, with an alpha of 0.05 and a power of 80%. The predicted sample size was 40 patients in both the migraine and healthy control groups (a total of 80 participants).

Statistical analysis was performed using SPSS software version 18 (SPSS Inc., Chicago, IL, USA). Continuous data are presented as means and standard deviations (SDs); categorical data are presented as frequencies and percentages. The paired t-test was used to compare the pRNFL, mRNFL, GCL, IPL, and INL thicknesses in each group, and independent t-tests for means of variables from different groups. The difference is expressed as a probability value (p-value) and was considered significant at <0.05. ANOVA and *post-hoc* analysis among control eyes, headache-side eyes, and non-headache-side eyes are performed. The correlation coefficients (r) from Pearson's correlation test were analyzed to assess the correlation between ThaiMIDAS scores, the frequency of attacks, and the thickness of all areas. The 95% confidence interval (95% CI) was computed using a bootstrap approach to correct for multiple comparisons in the correlation analysis.

RESULTS

We recruited 40 migraine patients and 40 healthy individuals for this study; two from each group were excluded due to poor image quality of the OCT, leaving 38 subjects in each group. Table 1 summarizes the demographic and clinical characteristics of the participants. The mean ages of the migraine patients and controls were 36.29 ± 9.45 and 36.45 ± 9.27 years, respectively. Thirty-four patients (89.48%) in both groups were female. The mean duration of migraine was 7.18 ± 6.05 years. The mean frequency of migraine attacks was

Table 1 Demographic data. The patients' demographic data; no parameters were significantly differ between controls and migraine patients.

Parameters		Mean	SD	*p*-value[*]
Age (year)	Control	36.45	9.273	0.942
	Migraine	36.29	9.449	
VA OD (LogMAR)	Control	0.150	0.2898	0.1340
	Migraine	0.065	0.1847	
VA OS (LogMAR)	Control	0.197	0.3217	0.0780
	Migraine	0.083	0.2201	
BMI (kg/m^2)	Control	22.480	3.1518	0.0550
	Migraine	24.060	3.8912	
IOP OD (mmHg)	Control	14.258	2.6726	0.2490
	Migraine	14.922	2.2517	
IOP OS (mmHg)	Control	14.042	2.4031	0.3898
	Migraine	14.881	3.5035	

Note:
[*] Independent t-test.

7.34 ± 7.65 times per month. The mean score of the Thai-MIDAS in migraine patients was 19.63 ± 20.44, and the majority were categorized as grade IV: severe disability (44.70%).

The mean thickness of the pRNFL, mRNFL, GCL, INL are displayed according to eye sides (left or right) in Table 2.

Data were evaluated firstly regarding the presence or absence of migraine. The mean thicknesses of the retinal layers from both eyes of the migraine group and controls are compared using an independent t-test as displayed in Table 3. Among the retinal layers studied in both groups, only one area, the superior-outer sector INL of migraine patients, was significantly thicker than controls, exhibiting 33.82 ± 2.46 μm *versus* 32.66 ± 2.34 μm, respectively (p = 0.039, t = 2.10 and degree of freedom = 74). For ease of orientation of each area and layer of the retina, the mean thickness of each layer is illustrated using Garway-Heath and ETDRS sectors with controls in Fig. 1, migraine cases by eye in Fig. 2, and migraine cases by headache-side or non-headache-side eyes in Fig. 3.

Further analysis considering the side of the headache in relation to the eye side was done by ANOVA and *post-hoc* analysis, comparing control eyes, headache-side eyes, and non-headache-side eyes showed reduced thickness of the GCL at temporal-outer sector and mRNFL at the superior-outer sector of the headache-side eyes when compared to that of control (mean difference 2.14 ± 1.04, p = 0.042, 95%CI [0.077–4.212]; mean difference 3.47 ± 1.64, p = 0.038, 95%CI [0.205–6.742], respectively).

When only patients with unilateral headaches were included, and thicknesses of the nasal and temporal sides of each eye were grouped in respect to the optic pathway, no significant difference of retinal layers between headache-side eyes, non-headache-side eyes, and controls were found.

Correlation analysis in Table 4 showed a low positive correlation between the Thai-MIDAS score and frequency of attacks (r = 0.495, p = 0.002, 95%CI [0.319–0.747]).

Table 2 Thickness of each layer and area (sector) of the retina of controls and migraine patients. The thickness of each sector of the retina from left and right eye of controls and migraine patients.

Layer and sector by eye			Thickness ± SD (µm)			
			Control		Migraine	
			Mean	Std. deviation	Mean	Std. deviation
pRNFL	Right eye	G	104.50	18.10	107.24	7.80
		T	79.71	12.36	78.24	14.98
		TS	147.18	18.24	147.16	17.41
		NS	114.37	16.52	119.95	21.15
		N	77.97	14.36	78.82	15.63
		NI	124.32	19.22	122.45	21.75
		TI	155.87	17.80	154.13	20.25
	Left eye	G	106.05	10.09	106.58	7.71
		T	79.13	12.42	77.47	14.49
		TS	148.34	21.27	146.39	19.15
		NS	125.26	18.67	133.00	22.50
		N	69.68	11.71	73.16	13.68
		NI	115.39	26.44	115.29	19.83
		TI	159.42	15.17	155.66	18.77
mRNFL	Right eye	Central	13.74	14.17	10.92	2.10
		T-inner	16.92	1.22	16.38	1.01
		S-inner	24.74	4.52	23.11	3.20
		N-inner	20.08	2.31	19.95	2.37
		I-inner	24.05	3.18	23.95	2.84
		T-outer	19.21	4.79	18.14	1.00
		S-outer	40.55	7.08	37.57	3.97
		N-outer	47.11	7.99	45.68	5.75
		I-outer	40.00	4.81	38.81	5.24
	Left eye	Central	11.39	2.34	11.16	2.26
		T-inner	16.29	0.93	16.26	1.20
		S-inner	24.11	3.48	22.84	3.25
		N-inner	19.84	2.16	19.37	1.70
		I-inner	22.79	3.36	23.26	2.50
		T-outer	17.92	1.24	18.74	4.68
		S-outer	39.45	7.00	37.37	4.78
		N-outer	46.53	6.14	43.55	7.29
		I-outer	39.21	4.97	38.32	5.03
GCL	Right eye	Central	13.53	3.96	11.76	2.99
		T-inner	45.84	5.25	46.22	4.72
		S-inner	52.61	3.97	52.32	3.56
		N-inner	51.39	4.51	50.73	3.81
		I-inner	50.76	5.09	51.43	3.25
		T-outer	37.84	4.04	36.76	3.72

(Continued)

Table 2 (continued)

Layer and sector by eye			Thickness ± SD (µm)			
			Control		**Migraine**	
			Mean	**Std. deviation**	**Mean**	**Std. deviation**
	Left eye	S-outer	36.03	3.13	36.89	3.67
		N-outer	40.45	3.42	40.49	3.45
		I-outer	34.79	3.80	34.51	2.73
		Central	13.34	4.04	12.37	4.04
		T-inner	46.68	4.44	46.24	3.89
		S-inner	52.13	3.93	52.45	3.57
		N-inner	49.84	4.89	50.63	3.99
		I-inner	50.55	5.34	50.61	4.40
		T-outer	36.87	3.59	36.47	4.51
		S-outer	35.68	3.14	36.18	3.40
		N-outer	40.97	3.71	41.34	3.42
		I-outer	35.39	3.69	35.05	3.61
INL	Right eye	Central	16.74	4.32	15.62	4.27
		T-inner	37.11	3.29	36.78	3.87
		S-inner	40.71	3.76	41.16	3.63
		N-inner	40.29	3.59	40.32	3.38
		I-inner	40.61	3.60	40.14	3.23
		T-outer	34.42	2.53	34.24	2.65
		S-outer	32.63	2.59	33.73	2.50
		N-outer	35.08	2.46	35.16	2.39
		I-outer	32.66	2.46	32.43	2.70
	Left eye	Central	16.39	4.27	15.71	4.79
		T-inner	37.76	2.93	37.26	3.67
		S-inner	41.66	3.68	40.79	3.56
		N-inner	39.34	3.97	39.34	3.29
		I-inner	40.39	4.04	40.47	3.58
		T-outer	34.08	2.26	33.92	2.28
		S-outer	32.68	2.34	33.92	2.61
		N-outer	35.71	3.05	35.68	3.20
		I-outer	33.16	2.97	32.74	2.71

Note:
G, global; T, temporal; TS, temporal-superior; NS, nasal-superior; N, nasal; NI, nasal-inferior; TI, temporal-inferior.

The severity scores also showed low positive correlations with the mRNFL thickness at the nasal-inner sector of the non-headache-side eyes (r = 0.448, p = 0.048, 95%CI [−0.310 to 0.781]), and moderate negative correlations with the INL thickness at the superior-outer sector of the headache-side eye (r = −0.509, p = 0.026, 95% CI [−0.770 to 0.014]).
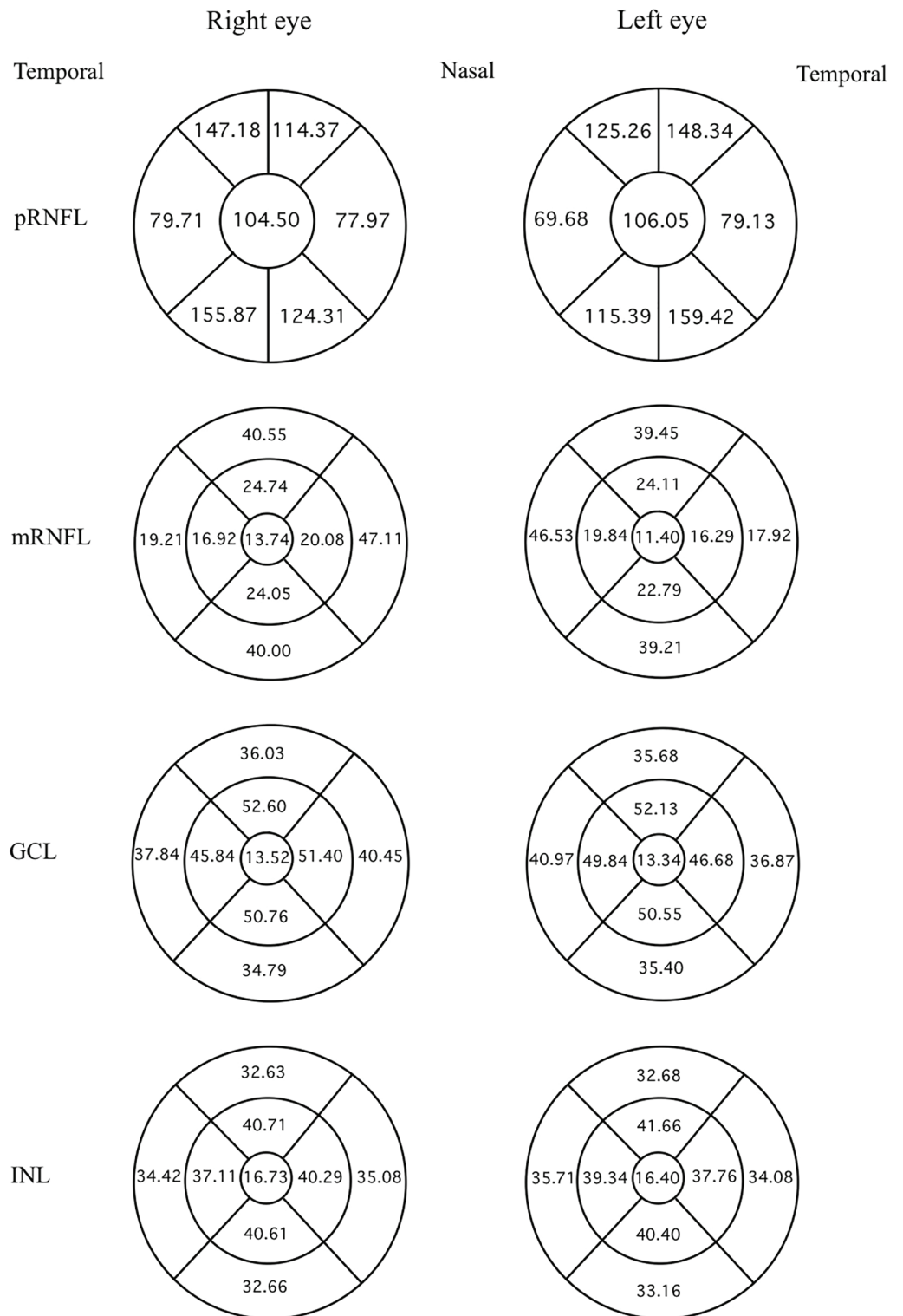
Table 3 Mean thicknesses of each retinal layers from both eyes of controls and migraine patients. The thickness of each retinal sector from both eyes in controls and migraine patients.

Layers and sectors both eyes		Thickness ± SD (μm)				df	t-Value	p-Value*
		Control		Migraine				
		Mean	Std. deviation	Mean	Std. deviation			
pRNFL	G	105.28	12.16	106.91	7.62	56	0.70	0.486
	T	79.42	11.95	77.86	13.53	56	0.54	0.594
	TS	147.76	18.97	146.78	17.03	56	0.24	0.812
	NS	119.82	16.21	126.47	20.88	56	1.56	0.125
	N	73.83	11.66	75.99	13.84	56	0.74	0.465
	NI	119.86	20.63	118.87	19.21	56	0.22	0.830
	TI	157.64	15.59	154.89	18.32	56	0.71	0.483
mRNFL	Central	12.57	7.03	11.01	1.99	56	1.30	0.200
	T-inner	16.61	0.81	16.32	0.95	56	1.38	0.172
	S-inner	24.42	3.61	23.00	2.82	56	1.90	0.062
	N-inner	19.96	1.98	19.68	1.77	56	0.66	0.514
	I-inner	23.42	2.80	23.62	2.18	56	0.35	0.731
	T-outer	18.57	2.50	18.45	2.47	56	0.21	0.835
	S-outer	40.00	6.84	37.45	4.19	56	1.95	0.056
	N-outer	46.82	6.52	44.58	5.96	56	1.55	0.126
	I-outer	39.61	4.58	38.58	4.89	56	0.94	0.352
GCL	Central	13.43	3.77	12.03	3.28	56	1.73	0.089
	T-inner	46.26	4.59	46.22	3.87	56	0.05	0.962
	S-inner	52.37	3.83	52.34	3.39	56	0.04	0.971
	N-inner	50.62	4.50	50.66	3.46	56	0.05	0.963
	I-inner	50.66	4.91	50.96	3.29	56	0.31	0.756
	T-outer	37.36	3.47	36.66	3.88	56	0.82	0.417
	S-outer	35.86	2.99	36.57	3.46	56	0.96	0.342
	N-outer	40.58	3.37	39.79	3.20	56	0.85	0.401
	I-outer	35.09	3.58	34.81	2.97	56	0.37	0.712
INL	Central	16.65	4.07	16.05	4.67	56	0.50	0.620
	T-inner	37.43	2.84	37.01	3.56	56	0.57	0.573
	S-inner	41.18	3.38	40.91	3.33	56	0.36	0.720
	N-inner	39.82	3.56	39.73	2.80	56	0.12	0.908
	I-inner	40.50	3.42	40.26	3.08	56	0.32	0.747
	T-outer	34.25	2.28	34.11	2.37	56	0.26	0.792
	S-outer	32.66	2.34	33.82	2.46	56	2.11	0.039
	N-outer	35.39	2.63	35.43	2.73	56	0.06	0.952
	I-outer	32.91	2.57	32.61	2.57	56	0.51	0.615

Notes:
*$p < 0.05$.
df, degree of freedom; G, global; T, temporal; TS, temporal-superior; NS, nasal-superior; N, nasal; NI, nasal-inferior; TI, temporal-inferior.

Figure 1 **Mean thicknesses of each sector of retinal layers by eye side in healthy controls.** Mean thicknesses of each sector of different retinal layers by eye side of healthy controls. First column displays the right eye, and second column the left. First row is the peripapillary retinal nerve fiber layer (pRNFL)

Udomwech et al. (2024), *PeerJ*, DOI 10.7717/peerj.17454

8/19

Figure 1 (continued)
in Garway-Heath sector, inner circle shows the global average, the circumferential sectors from inner (nasal) are the inner, inner-superior, temporal-superior, temporal, temporal-inferior, and nasal-inferior sectors of the pRNFL, respectively, anti-clockwise for the right eye, clockwise for the left. From the second row, ETDRS map was used: the innermost circle shows the foveal thickness. The middle circumferential sectors, starting from the nasal side are the nasal-inner, superior-inner, temporal-inner, and inferior-inner sectors, respectively, anti-clockwise for the right eye and clockwise for the left. The outermost circumferential sectors, starting from the nasal side, are the nasal-outer, superior-outer, temporal-outer, and inferior-outer sectors of the macular retinal layers, respectively, anti-clockwise for the right eye, and clockwise for the left eye.   Full-size 🖼 DOI: 10.7717/peerj.17454/fig-1

DISCUSSION

Evaluation of mean RNFL (peripapillary and macular) thickness from both eyes of migraine patients in our study has found no significant reduction compared to controls. Extended investigation to other retinal structures, including GCL and INL, according to the hypothesis that these layers of the retina might constitute more appropriate morphological parameters for axonal damage than RNFL (*Yener & Korucu, 2019*), found significant thickening of the superior-outer sector of the INL in migraine patients compared to controls. Furthermore, we observed a significant thinning of the GCL at temporal-outer sector and mRNFL at the superior-outer sector of the headache-side eyes when compared to that of control eyes.

The results of RNFL thickness in migraine patients of our study were contrary to previous studies (*Demircan et al., 2015*; *Acer et al., 2016*; *Gunes et al., 2018*; *Sirakaya et al., 2020*; *Ao et al., 2018*; *Abdellatif & Fouad, 2018*; *Gipponi et al., 2013*; *Martinez, Proupim & Sanchez, 2009*; *Yülek et al., 2015*; *Sorkhabi et al., 2013*; *Reggio et al., 2017*; *Tak, Sengul & Bilak, 2018*; *Feng et al., 2016*), systematic reviews, and meta-analyses, in which RNFL thickness was thinner in the migraine group than in the control group, most significantly in the superior and inferior quadrants (*Lin et al., 2021*). However, RNFL parameters may change more in migraine with aura than in migraine without aura (*El-Shazly et al., 2017*; *Ekinci et al., 2014*; *Ulusoy, Horasanli & Kal, 2019*). It has been speculated that when migraine attacks, changes of the optic nerve and RNFL blood supply may lead to hypoxic injury, which in turn leads to the death of retinal ganglion cells (*Ao et al., 2018*). Transneuronal retrograde degeneration (TRD), *i.e.*, the degeneration of a target neuron after the death of the presynaptic neuron or loss of presynaptic input, occurs in most neurons in both the infantile and adult central nervous systems. TRD has been observed after pathological damage to the central and peripheral nervous systems. There is also evidence of atrophy of ipsilateral retinal ganglion cells after occipital lobectomy in animals. *Park et al. (2013)* demonstrated that the RNFL was reduced in patients with cerebral infarction, providing evidence for TRD in retinal ganglion cells. Therefore, repeated onsets of migraine could result in the alteration of the structure and function of the occipital lobe (*Cowey, Alecxander & Stoerig, 2011*) as a subsequent change to retinal structures. *Yener & Korucu (2019)* and *Simsek, Aygun & Yildiz (2015)* reported no significant difference in RNFL measurements between patients and controls, which is similar to our study. These distinct results may be explained with the use of different methods and sample sizes, racial
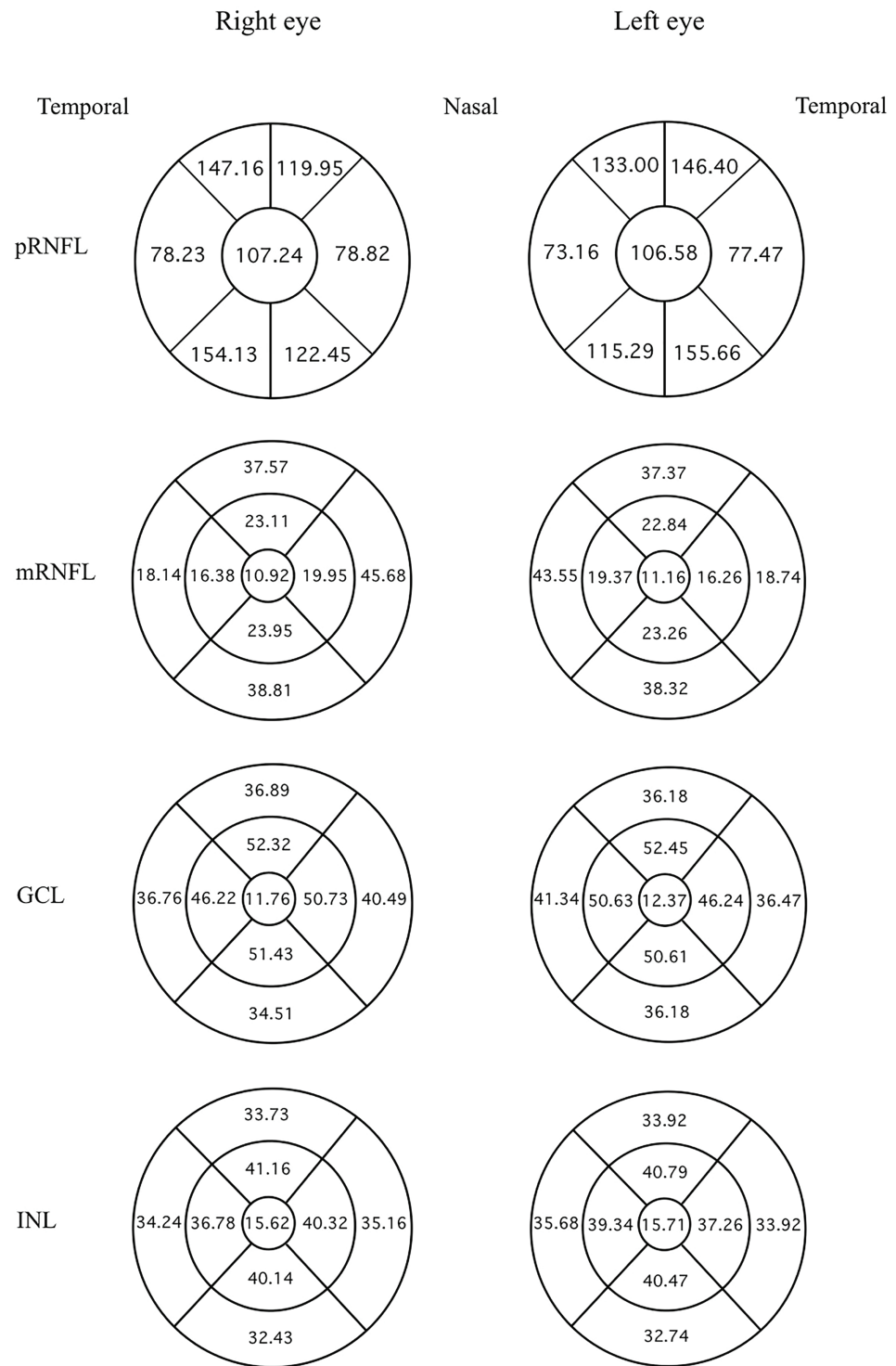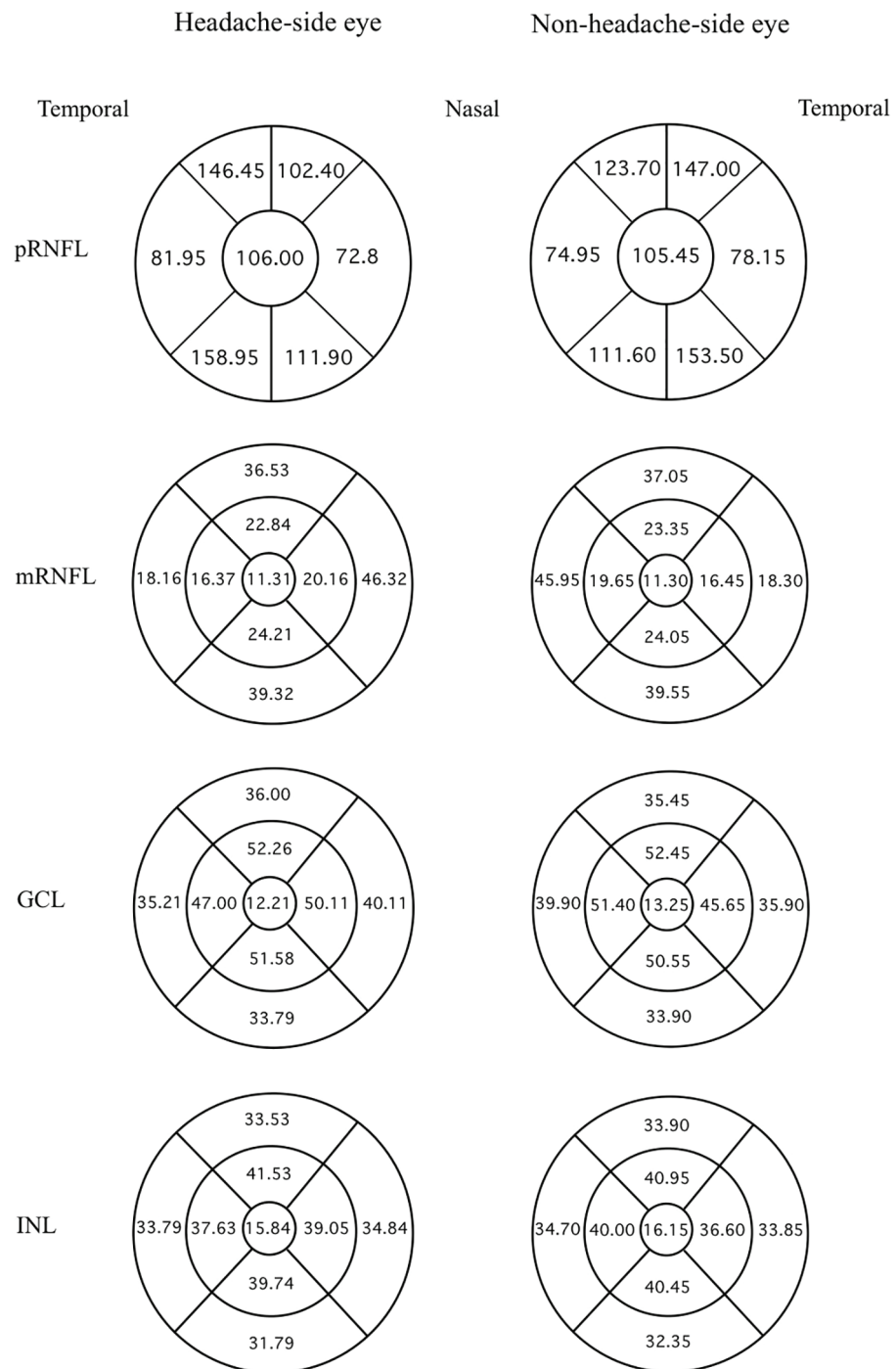
Figure 2 Mean thicknesses of each sector of retinal layers by eye side in migraine patients. Mean thicknesses of each sector of different retinal layers by eye side of migraine patients. The first column displays the right eye, the second column shows the left eye. Each row represents different location or layers measured. Full-size 🖼 DOI: 10.7717/peerj.17454/fig-2

Cases: Eyes in Respect of Headache Side

Figure 3 Mean thicknesses of each sector of retinal layers of the headache side eye and non-headache-side eye. Mean thicknesses of each sector of different retinal layers of the headache side eye (1st column) and non-headache-side eye (2nd column). Please note that this figure represents the mean of the headache-side/non-headache-side eyes disregarding to the eye side. The headache-side eyes are shown in a diagram of the right eye, and non-headache-side eyes in a diagram of the left eye, this is for the readers' ease of orientation of the retinal sectors.   Full-size 🖾 DOI: 10.7717/peerj.17454/fig-3

Table 4 Correlation between Thai-MIDAS score and RNFL thickness. The correlation between severity of migraine which evaluated by Thai-MIDAS score and the thickness of each retinal sector.

Parameters	Thai-MIDAS score						
	Pearson correlation (r)	*p*-value (2-tailed)	N	Bootstrap[c]			
				Bias	Std. error	95% Confidence interval	
						Lower	Upper
Frequency (times/mo)	0.495**	0.002	38	0.028	0.115	0.316	0.763
IpRNFLG	−0.155	0.515	20	0.008	0.158	−0.431	0.175
CpRNFLG	−0.049	0.837	20	−0.015	0.168	−0.438	0.260
IpRNFLT	−0.053	0.825	20	−0.036	0.253	−0.516	0.466
CpRNFLT	0.177	0.455	20	−0.020	0.237	−0.317	0.608
IpRNFLTS	−0.166	0.484	20	0.006	0.224	−0.516	0.311
CpRNFLTS	0.204	0.388	20	−0.046	0.245	−0.501	0.513
IpRNFLNS	−0.062	0.794	20	0.036	0.218	−0.381	0.455
CpRNFLNS	−0.099	0.679	20	−0.047	0.239	−0.672	0.242
IpRNFLN	−0.047	0.843	20	−0.008	0.219	−0.460	0.357
CpRNFLN	−0.023	0.924	20	0.002	0.215	−0.410	0.395
IpRNFLIN	−0.139	0.558	20	0.069	0.287	−0.546	0.477
CpRNFLNI	−0.302	0.195	20	0.033	0.223	−0.613	0.243
IpRNFLTI	−0.065	0.787	20	−0.045	0.202	−0.550	0.256
CpRNFLTI	−0.070	0.768	20	−0.022	0.155	−0.473	0.180
Innervating pRNFL	−0.167	0.481	20	−0.011	0.159	−0.516	0.140
Non-innervating pRNFL	0.027	0.909	20	0.009	0.162	−0.256	0.383
ImRNFLcen	0.136	0.578	19	0.039	0.197	−0.168	0.641
CmRNFLcen	0.223	0.360	19	0.025	0.167	−0.093	0.575
ImRNFLTinn	−0.074	0.762	19	0.011	0.183	−0.423	0.325
CmRNFLTinn	−0.295	0.221	19	0.034	0.236	−0.618	0.312
ImRNFLTSinn	0.001	0.995	19	−0.033	0.207	−0.489	0.303
CmRNFLTSinn	0.245	0.313	19	−0.068	0.292	−0.428	0.627
ImRNFLNinn	0.156	0.522	19	−0.007	0.184	−0.276	0.503
CmRNFLNinn	0.448*	0.048	20	−0.072	0.307	−0.305	0.780
ImRNFLIinn	0.259	0.284	19	−0.015	0.216	−0.208	0.658
CmRNFLIinn	−0.415	0.069	20	0.086	0.315	−0.769	0.381
ImRNFLTout	−0.225	0.354	19	−0.020	0.176	−0.624	0.126
CmRNFLTout	−0.361	0.129	19	0.018	0.190	−0.659	0.102
ImRNFLSout	−0.017	0.945	19	−0.040	0.226	−0.616	0.298
CmRNFLSout	−0.040	0.872	19	−0.048	0.247	−0.660	0.320
ImRNFLNout	0.056	0.819	19	−0.047	0.245	−0.510	0.408
CmRNFLNout	0.164	0.502	19	−0.097	0.356	−0.609	0.604
ImRNFLIout	−0.151	0.538	19	−0.040	0.196	−0.585	0.177
CmRNFLIout	−0.195	0.424	19	−0.054	0.212	−0.660	0.156
Innervating mRNFL	0.102	0.679	19	−0.066	0.298	−0.567	0.488
Non-innervating mRNFL	−0.072	0.771	19	0.035	0.206	−0.382	0.415

Table 4 (continued)

Parameters	Thai-MIDAS score						
	Pearson correlation (r)	*p*-value (2-tailed)	N	Bootstrap[c]			
				Bias	Std. error	95% Confidence interval	
						Lower	Upper
IGCLcen	0.142	0.561	19	0.045	0.172	−0.127	0.557
CGCLcen	0.446	0.056	19	−0.022	0.206	−0.022	0.792
IGCLTinn	0.275	0.255	19	−0.046	0.260	−0.304	0.687
CGCLTinn	−0.122	0.617	19	−0.035	0.201	−0.633	0.201
IGCLTSinn	0.183	0.453	19	−0.057	0.249	−0.474	0.525
CGCLTSinn	0.163	0.506	19	-0.088	0.328	−0.670	0.595
IGCLNinn	0.136	0.578	19	−0.035	0.211	−0.340	0.443
CGCLNinn	0.338	0.157	19	−0.096	0.339	−0.464	0.745
IGCLIinn	0.216	0.374	19	−0.113	0.367	−0.603	0.685
CGCLIinn	−0.220	0.365	19	−0.028	0.190	−0.646	0.132
IGCLTout	0.205	0.401	19	−0.118	0.356	−0.600	0.627
CGCLTout	0.041	0.866	19	−0.062	0.279	−0.537	0.478
IGCLSout	−0.235	0.333	19	−0.076	0.193	−0.699	0.033
CGCLSout	−0.300	0.212	19	−0.051	0.137	−0.641	−0.107
IGCLNout	−0.140	0.567	19	−0.026	0.154	−0.517	0.122
CGCLNout	−0.197	0.420	19	−0.015	0.166	−0.561	0.140
IGCLIout	−0.066	0.788	19	−0.053	0.214	−0.616	0.238
CGCLIout	0.346	0.147	19	−0.151	0.412	−0.653	0.774
Innervating GCL	0.099	0.686	19	−0.081	0.316	−0.620	0.549
Non-innervating GCL	−0.040	0.870	19	−0.067	0.270	−0.639	0.365
IINLcen	0.019	0.940	19	0.045	0.242	−0.376	0.570
CINLcen	0.167	0.494	19	0.021	0.159	−0.096	0.525
IINLTinn	−0.090	0.715	19	−0.001	0.166	−0.398	0.291
CINLTinn	−0.204	0.402	19	−0.004	0.173	−0.504	0.183
IINLTSinn	−0.310	0.197	19	0.002	0.199	−0.625	0.204
CINLTSinn	−0.036	0.883	19	−0.001	0.189	−0.410	0.350
IINLNinn	−0.119	0.627	19	0.0058	0.245	−0.413	0.534
CINLNinn	−0.082	0.739	19	0.014	0.187	−0.384	0.373
IINLIinn	0.037	0.880	19	−0.004	0.169	−0.306	0.361
CINLIinn	−0.241	0.321	19	0.0013	0.230	−0.634	0.257
IINLTout	−0.170	0.486	19	−0.035	0.169	−0.577	0.101
CINLTout	−0.040	0.870	19	−0.010	0.166	−0.436	0.280
IINLSout	−0.509*	0.026	19	0.030	0.197	−0.746	0.067
CINLSout	−0.398	0.091	19	0.022	0.215	−0.742	0.136
IINLNout	−0.192	0.430	19	0.013	0.222	−0.580	0.330
CINLNout	−0.136	0.579	19	−0.015	0.157	−0.459	0.161
IINLIout	−0.200	0.411	19	0.005	0.201	−0.572	0.250

(Continued)

	Thai-MIDAS score						
Parameters	**Pearson correlation (r)**	**p-value (2-tailed)**	**N**	**Bootstrap[c]**			
				Bias	**Std. error**	**95% Confidence interval**	
						Lower	**Upper**
CINLIout	0.047	0.849	19	−0.044	0.246	−0.543	0.418
Innervating INL	−0.151	0.537	19	−0.013	0.155	−0.468	0.159
Non-innervating INL	−0.193	0.429	19	0.005	0.216	−0.546	0.352

Table 4 (continued)

Notes:
* Correlation is significant at the 0.05 level (2-tailed).
** Correlation is significant at the 0.01 level (2-tailed).
[c] Unless otherwise noted, bootstrap results are based on 1,000 bootstrap samples.
I, headache-side eye; C, non-headache-side eye; Cen, center; Inn, inner; Out, outer; G, global; T, temporal; TS, temporal-superior; NS, nasal-superior; N, nasal; NI, nasal-inferior; TI, temporal-inferior.

differences, and the variation of migraine parameters such as severity of headache, duration of headache, duration of attack, and frequency of attacks.

The extended investigation of INL layer in our results found significant thickening of the superior-outer sector in migraine patients compared to controls. The INL is composed of three neuronal cell classes (horizontal, bipolar, and amacrine cells) and one class of glia (Müller cells). Müller cell dysfunction in the fovea has been specifically linked to degenerative diseases affecting the macula (*Masri et al., 2021*). The INL is mostly studied in central demyelinating diseases, multiple sclerosis, and neuromyelitis optica (*Balk et al., 2019*; *Cellerino et al., 2019*; *Gelfand et al., 2013*). *Balk et al. (2019)* demonstrated the relationship between the thickening of the INL, physical disability, and disease activity in multiple sclerosis. The underlying mechanism responsible for the thickening of the INL remains unknown. The INL is embedded between the superficial vascular plexus and the deep capillary plexus, whereas both plexuses and Müller cells can absorb the interstitial fluid. One suggested mechanism involves inflammation-related dynamic fluid shifts (*Spaide, 2016*). Dynamic retinal layer volume changes can be explained by fluid shifts due to a combination of osmotic and hydrostatic gradients in the retinal lymphatic system (*Petzold, 2016*). In the process of inflammation, diffusion of fluid from the retinal blood vessels increases, leading to an increase in INL thickness. Therefore, this finding supports that inflammation might be involved in the pathophysiology of migraine, leading to thickening of the INL. Moreover, Müller cell dysfunction can result from TRD. Another suggested mechanism is the pathology of Müller cells, which would impair the absorption of interstitial fluid, also resulting in increased INL thickness (*Lujan & Horton, 2013*).

Our study evaluated specifically in unilateral headache migraine, by observed the changed in retinal structural in headache-side eyes compared to contralateral-eyes and controls. There were significantly reduced in thickness of the GCL at temporal-outer sector and mRNFL at the superior-outer sector of the headache-side eyes. There was only one study which mention of lateralization of headache and RNFL thickness (*Gunes et al., 2016*). *Gunes et al. (2016)* investigated the relationship between migraine headache

lateralization and RNFL thickness in migraine patients with unilateral headache. They found the thinning of RNFL was higher on the side of the headache compared to the contralateral side, but the difference was not statistically significant. So, our study is the first study that found the significant relation of RNFL thinning on the headache-side eye. These results may explained by the reduction of blood flow and vasospasm during migraine episodes which usually occur in one hemisphere (*Killer, Forrer & Flammer, 2003*). There are some studies of unilateral involvement in migraine patients (*Friberg et al., 1991*; *Hougaard et al., 2015*). *Friberg et al. (1991)* found reduced blood flow velocities in the middle cerebral artery on the affected side during migraine episodes. *Hougaard et al. (2015)* identified thinning of the ipsilateral hemisphere cortical thickness in the inferior frontal gyrus. The finding of more prominent thinning in some part RNFL and GCL in headache-side eye might be related with lateralized structural abnormalities in the cortex, indicating that the hemisphere on the side of pain is affected more.

The positive correlation between the Thai-MIDAS score and frequency of attacks, although not surprising, affirms the nature of the disease. The correlation between the duration of migraine history, attack frequency, were not clear, like several studies that did not find any correlation similar to ours (*Simsek, Aygun & Yildiz, 2015*; *Labib et al., 2020*); nevertheless, inverse correlations have also been reported (*Acer et al., 2016*; *Martinez, Proupim & Sanchez, 2009*; *Reggio et al., 2017*; *Gunes et al., 2016*). Interestingly, our data showed a negative correlation between INL in the superior outer sector of the headache-side eyes despite being the only area showing significantly increased thickness when compared to controls. Although it seemed counterintuitive that the INL of the headache-side eyes negatively correlated with the disability scores, it may be explainable. In early or mild severity migraine, the pathogenesis could be explained by the transneuronal retrograde degeneration (TRD) that may cause cellular and interstitial inflammation and edema, most likely starting at the Müller cell, which was previously reported in multiple sclerosis and neuromyelitis optica, resulting in increased INL thickness (*Balk et al., 2019*; *Cellerino et al., 2019*; *Gelfand et al., 2013*; *Lujan & Horton, 2013*). On the contrary, in more severe migraine with higher disability scores, the TRD is more chronic and result in cellular loss and atrophy, resulting in thinner INL. However, these discrepant outcomes may also have been due to incidental variations in the studied population. The relationships between INL thickness and migraine headache variables should be studied further.

This study still possesses some limitations. A larger multi-center study should be beneficial to show stronger proof of eye-brain interaction of migraine.

CONCLUSIONS

The thickness of the superior outer subfield of INL was significantly thicker in migraine patients than in healthy subjects. This finding may be related to the inflammation and Müller cell dysfunction that occurs in migraine. There was significant thinning of the GCL at temporal-outer sector and mRNFL at the superior-outer sector of the headache-side eyes which may related to headache lateralization, focal vasospasm and cortical changed. Correlation showed a positive correlation between the Thai-MIDAS score and frequency

of attacks, the nasal-inner mRNFL thickness, of the non-headache-side eyes, but negative correlations with the superior-outer INL thickness of the headache-side eyes.

ADDITIONAL INFORMATION AND DECLARATIONS

Competing Interests

The authors declare that they have no competing interests.

Author Contributions

- Lunla Udomwech conceived and designed the experiments, performed the experiments, analyzed the data, prepared figures and/or tables, authored or reviewed drafts of the article, and approved the final draft.
- Rini Sulastiwaty analyzed the data, authored or reviewed drafts of the article, and approved the final draft.
- Doungkamol Siriarchawawat conceived and designed the experiments, performed the experiments, analyzed the data, prepared figures and/or tables, authored or reviewed drafts of the article, and approved the final draft.

Human Ethics

The following information was supplied relating to ethical approvals (*i.e.*, approving body and any reference numbers):
Walailak Ethics Committee.

Data Availability

The following information was supplied regarding data availability:
The raw data is available in the Supplemental File.

Supplemental Information

Supplemental information for this article can be found online at http://dx.doi.org/10.7717/peerj.17454#supplemental-information.

REFERENCES

Abdellatif MK, Fouad MM. 2018. Effect of duration and severity of migraine on retinal nerve fiber layer, ganglion cell layer, and choroidal thickness. *European Journal of Ophthalmology* **28(6)**:714–721 DOI 10.1177/1120672117750054.

Abdul-Rahman AM, Gilhotra JS, Selva D. 2011. Dynamic focal retinal arteriolar vasospasm in migraine. *Indian Journal of Ophthalmology* **59(1)**:51–53 DOI 10.4103/0301-4738.73717.

Acer S, Oguzhanoglu A, Cetin EN, Yağcı R, Yıldırım C, Ağladıoğlu SY, Özhan B. 2016. Ocular pulse amplitude and retinal nerve fiber layer thickness in migraine patients without aura. *BMC Ophthalmology* **16**:1 DOI 10.1186/s12886-015-0180-2.

Ao R, Wang R, Yang M, Wei S, Shi X, Yu S. 2018. Altered retinal nerve fiber layer thickness and choroid thickness in patients with migraine. *European Neurology* **80(3–4)**:130–137 DOI 10.1159/000494671.

Balk LJ, Coric D, Knier B, Zimmermann HG, Behbehani R, Alroughani R, Martinez-Lapiscina EH, Brandt AU, Sánchez-Dalmau B, Vidal-Jordana A, Albrecht P, Koska V, Havla J, Pisa M, Nolan RC, Leocani L, Paul F, Aktas O, Montalban X, Balcer LJ, Villoslada P, Outteryck O, Korn T, Petzold A, On behalf of the IMSVISUAL consortium. 2019. Retinal inner nuclear layer volume reflects inflammatory disease activity in multiple sclerosis; a longitudinal OCT study. *Multiple Sclerosis Journal-Experimental, Translational and Clinical* **5(3)**:2055217319871582 DOI 10.1177/2055217319871582.

Cellerino M, Cordano C, Boffa G, Bommarito G, Petracca M, Sbragia E, Novi G, Lapucci C, Capello E, Uccelli A, Inglese M. 2019. Relationship between retinal inner nuclear layer age, and disease activity in progressive MS. *Neurology Neuroimmunology & Neuroinflammation* **6(5)**:e596 DOI 10.1212/NXI.0000000000000596.

Cowey A, Alecxander I, Stoerig P. 2011. Transneuronal retrograde degeneration of retinal ganglion cells and optic tract in hemianopic monkeys and humans. *Brain* **134(Pt 7)**:2149–2157 DOI 10.1093/brain/awr125.

Demircan S, Ataş M, Arık Yüksel S, Ulusoy MD, Yuvacı İ, Arifoğlu HB, Başkan B, Zararsız G. 2015. The impact of migraine on posterior ocular structures. *Journal of Ophthalmology* **2015(10)**:868967–868968 DOI 10.1155/2015/868967.

Ekinci M, Ceylan E, Çağatay HH, Keleş S, Hüseyinoğlu N, Tanyıldız B, Çakıcı Ö, Kartal B. 2014. Retinal nerve fiber layer, ganglion cell layer and choroid thinning in migraine with aura. *BMC Ophthalmology* **14(1)**:75 DOI 10.1186/1471-2415-14-75.

El-Shazly AAE-F, Farweez YA, Hamdi MM, EL-Sherbiny NE. 2017. Pattern visual evoked potential, pattern electroretinogram, and retinal nerve fiber layer thickness in patients with migraine during and after aura. *Current Eye Research* **42(9)**:1327–1332 DOI 10.1080/02713683.2017.1319490.

Feng Y-F, Guo H, Huang J-H, Yu J-G, Yuan F. 2016. Retinal nerve fiber layer thickness changes in migraine: a meta-analysis of case-control studies. *Current Eye Research* **41(6)**:814–822 DOI 10.3109/02713683.2015.1056373.

Friberg L, Sperling B, Olesen J, Iversen HK. 1991. Migraine pain associated with middle cerebral artery dilatation: reversal by sumatriptan. *Lancet* **338(8758)**:13–17 DOI 10.1016/0140-6736(91)90005-A.

Gelfand JM, Cree BA, Nolan R, Arnow S, Green AJ. 2013. Microcystic inner nuclear layer abnormalities and neuromyelitis optica. *JAMA Neurology* **70(5)**:629–633 DOI 10.1001/jamaneurol.2013.1832.

Gipponi S, Scaroni N, Venturelli E, Forbice E, Rao R, Liberini P, Padovani A, Semeraro F. 2013. Reduction in retinal nerve fiber layer thickness in migraine patients. *Neurological Sciences* **34(2)**:841–845 DOI 10.1007/s10072-012-1103-0.

Gunes A, Demirci S, Tok L, Tok O, Demirci S, Kutluhan S. 2016. Is retinal nerve fiber layer thickness change related to headache lateralization in migraine? *Korean Journal of Ophthalmology* **30(2)**:134–139 DOI 10.3341/kjo.2016.30.2.134.

Gunes A, Karadag AS, Yazgan S, Celik HU, Simsek K. 2018. Evaluation of retinal nerve fiber layer, ganglion cell layer and choroidal thickness with optical coherence tomography in migraine patients: a case-control study. *Clinical & Experimental Optometry* **101(1)**:109–115 DOI 10.1111/cxo.12585.

Headache Classification Committee of the International Headache Society (IHS). 2013. The international classification of headache disorders, 3rd edition (beta version). *Cephalalgia: An International Journal of Headache* **33(9)**:629–808 DOI 10.1177/0333102413485658.

Headache Classification Committee of the International Headache Society. 2018. The international classification of headache disorders. *Cephalalgia* **38(1)**:1–211 DOI 10.1177/0333102417738202.

Hougaard A, Amin FM, Hoffmann MB, Larsson HBW, Magon S, Sprenger T, Ashina M. 2015. Structural gray matter abnormalities in migraine relate to headache lateralization, but not aura. *Cephalalgia* **35(1)**:3–9 DOI 10.1177/0333102414532378.

Killer HE, Forrer A, Flammer J. 2003. Retinal vasospasm during an attack of migraine. *Retina* **23(2)**:253–254 DOI 10.1097/00006982-200304000-00023.

Labib DM, Hegazy M, Esmat SM, Ali EAH, Talaat F. 2020. Retinal nerve fiber layer and ganglion cell layer changes using optical coherence tomography in patients with chronic migraine: a case-control study. *The Egyptian Journal of Neurology, Psychiatry and Neurosurgery* **56(1)**:86 DOI 10.1186/s41983-020-00218-8.

Lin XG, Yi ZQ, Zhang XL, Liu QQ, Zhang H, Cai RY, Chen CC, Zhang HJ, Zhao PW, Pan PL. 2021. Retinal nerve fiber layer changes in migraine: a systematic review and meta-analysis. *Neurological Sciences* **42(3)**:871–881 DOI 10.1007/s10072-020-04992-4.

Lujan BJ, Horton JC. 2013. Microcysts in the inner nuclear layer from optic atrophy are caused by retrograde trans-synaptic degeneration combined with vitreous traction on the retinal surface. *Brain* **136(Pt11)**:e260 DOI 10.1093/brain/awt154.

Martinez A, Proupim N, Sanchez M. 2009. Scanning laser polarimetry with variable corneal compensation in migraine patients. *Acta Ophthalmologica* **87(7)**:746–753 DOI 10.1111/j.1755-3768.2008.01356.x.

Masri RA, Weltzien F, Purushothuman S, Lee SCS, Martin PR, Grünert U. 2021. Composition of the inner nuclear layer in human retina. *Investigative Opthalmology & Visual Science* **62(9)**:22 DOI 10.1167/iovs.62.9.22.

Park H-YL, Park YG, Cho A-H, Park CK. 2013. Transneuronal retrograde degeneration of the retinal ganglion cells in patients with cerebral infarction. *Ophthalmology* **120(6)**:1292–1299 DOI 10.1016/j.ophtha.2012.11.021.

Petzoid A. 2016. Retinal glymphatic system: an explanation for transient retinal layer volume changes? *Brain* **139(11)**:2816–2819 DOI 10.1093/brain/aww239.

Phanthumchinda K, Sithi-Amorn C. 1989. Prevalence and clinical features of migraine: a community survey in Bangkok, Thailand. *Headache* **29(9)**:594–597 DOI 10.1111/j.1526-4610.1989.hed2909594.x.

Reggio E, Chisari CG, Ferrigno G, Patti F, Donzuso G, Sciacca G, Avitabile T, Faro S, Zappia M. 2017. Migraine causes retinal and choroidal structural changes: evaluation with ocular coherence tomography. *Journal of Neurology* **264(3)**:494–502 DOI 10.1007/s00415-016-8364-0.

Russo A, Tessitore A, Tedeschi G. 2013. Migraine and trigeminal system-I can feel it coming. *Current Pain and Headache Reports* **17(10)**:367 DOI 10.1007/s11916-013-0367-2.

Simsek IB, Aygun D, Yildiz S. 2015. Retinal nerve fibe layer thickness in migraine patients with or without aura. *Neuro-Ophthalmology* **39(1)**:17–21 DOI 10.3109/01658107.2014.968740.

Sirakaya E, Kucuk B, Agadayi A, Yilmaz N. 2020. Evaluation of the lamina cribosa thickness and depth in patients with migraine. *International Ophthalmology* **40(1)**:89–98 DOI 10.1007/s10792-019-01160-2.

Sorkhabi R, Mostafaei S, Ahoor M, Talebi M. 2013. Evaluation of retinal nerve fiber layer thickness in migraine. *Iranian Journal of Neurology* **12(2)**:51–55.

Spaide RF. 2016. Retinal vascular cystoid macular edema: review and new theory. *Retina* **36(10)**:1823–1842 DOI 10.1097/IAE.0000000000001158.

Tak AZA, Sengul Y, Bilak S. 2018. Evaluation of white matter hyperintensities and retinal fiber layer, ganglion cell layer, inner plexiform layer, and choroidal layer in migraine patients. *Neurological Sciences* **39(3)**:489–496 DOI 10.1007/s10072-017-3234-9.

Tunç A, Güngen BD, Evliyaoğlu F, Aras YG, Tekeşin AK. 2017. Evaluation of retinal nerve fiber layer, ganglion cell layer and macular changes in patients with migraine. *Acta Neurologica Belgica* **117(1)**:121–129 DOI 10.1007/s13760-016-0715-1.

Ulusoy MO, Horasanli B, Kal A. 2019. Retinal vascular density evaluation of migraine patients with and without aura and association with white matter hyperintensities. *Acta Neurologica Belgica* **119(3)**:411–417 DOI 10.1007/s13760-019-01094-7.

Vongvaivanich K, Yongprawat T, Jindawong N, Chansakul C. 2018. Test-Restest reliablitiy of the Thai migraine disability assessment (Thai-MIDAS) questionnaire in Thai migraine patients. *The Bangkok Medical Journal* **14(1)**:10–15 DOI 10.31524/bkkmedj.2018.02.003.

Yener AU, Korucu O. 2019. Quantitative analysis of the retinal nerve fiber layer, ganglion cell layer and optic disc parameters by the swept source optical coherence tomography in patients with migraine and patients with tension-type headache. *Acta Neurologica Belgica* **119(4)**:541–548 DOI 10.1007/s13760-018-1041-6.

Yülek F, Dirik EB, Eren Y, Simavlı H, Uğurlu N, Çağıl N, Şimşek Ş. 2015. Macula and retinal nerve fiber layer in migraine patients: analysis by spectral domain optic coherence tomography. *Seminars in Ophthalmology* **30(2)**:124–128 DOI 10.3109/08820538.2013.833270.